Iterative Phasing of Coherent Diffractive Imaging

G.J. Williams, M.A. Pfeifer, I.K. Robinson
Department of Physics, University of Illinois at Urbana-Champaign, Urbana, IL, U.S.A.

Introduction

The coherent x-ray beam produced by the APS makes the measurement of 3-D coherent x-ray diffraction (CXD) patterns practical. Such patterns generated by a small, single crystal contain sufficient information to support the use of iterative algorithms to recover the 3-D diffracting density [1]. By using a Bragg reflection geometry, no special care needs to be taken to block the direct beam, and the sample needs to be rocked only a small amount to move the 3-D diffracted intensity through the 2-D detector. Additionally, higher-order Bragg peaks may be used to enhance the sensitivity to strain within the sample, promising the possibility to image strain within the sample in 3-D.

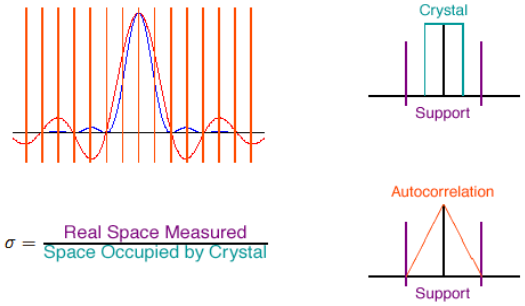

FIG. 1. The measured intensity must be sampled at the Nyquist frequency of the autocorrelation, at least twice as finely as the Nyquist rate for sampling the amplitude.

Methods and Materials

The sample discussed here is a Pb film, heated *in vacuo* to form single crystals less than 1 μm in diameter. The coherent diffraction hutch at sector 34 at the APS has been used to prepare the sample and measure diffraction near a {111} Bragg peak of such crystals. To acquire a 3-D pattern, the sample is rocked through the Bragg condition, and the resulting diffraction is measured with a 2-D charge-coupled device (CCD) detector, where sample rotation moves the diffracted intensity through the detector, providing the third dimension.

Since the measurement is one of intensity and not amplitude, it must be oversampled (Fig. 1). This is required because in order to invert a complex signal, it must be measured at the Nyquist frequency.

The actual intensity measurement is of the autocorrelation of the complex amplitude; therefore, we must oversample the intensity measurement to obtain enough information to reconstruct the amplitude we seek to invert, resulting in a 3-D density map in real space.

Once we have made the oversampled measurement, we rely on iterative algorithms to find the phase set that is consistent with the measured intensity. This is a difficult problem, but in two and higher dimensions, a unique solution should exist. The primary algorithm used is Feinup's error reduction [2], illustrated in Fig. 2. We

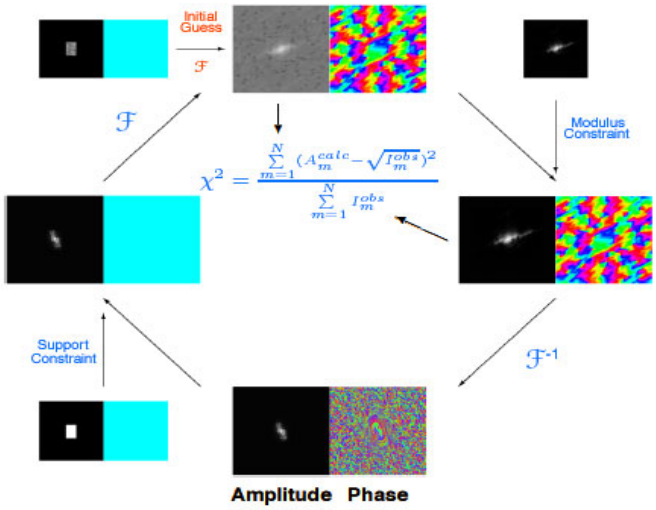

FIG. 2. A schematic diagram of the error reduction algorithm. Each fit begins with a random phase set and is iterated until a satisfactory solution is found.

begin each fit with a set of random phases and a finite support region, which is derived from knowledge about the sample (e.g., the crystal is compact in real space). A fast Fourier transform (FFT) is applied to this density, and we constrain the magnitudes of the reconstructed diffraction amplitudes to be those that were measured. The prospective solution is transformed back to real space by an inverse FFT, where it is constrained to have no phase gradient (since the crystal is expected to be unstrained) and to be compact. This set of densities is then transformed back to reciprocal space, and the cycle is repeated until a satisfactory solution is reached. The progress of the fit is recorded by the average rms error per pixel calculated with the reconstructed complex amplitude and the measured diffraction data during each iteration.

Results

Once the measured magnitude of the diffracted amplitude is phased, the complex diffraction amplitude can be readily transformed to a real space density by means of one last FFT. The result of several hundred iterations of the algorithm described above, applied to 2-D data, is shown in Fig. 3, with the original measured 2-D CXD pattern. In 3-D, the full 3-D CXD pattern is measured, which results in a 3-D real space density. In 2-D, one slice through the 3-D diffracted amplitude is recovered, and the transformation to real space is a projection of the density of the diffracting crystal onto a plane determined by the choice of the 2-D slice extracted from the 3-D CXD pattern.

The reconstructed real space density reveals a crystal with dimensions projected to be 1 μm by 0.6 μm, well within the range of crystal sizes shown to exist by *ex situ* scanning electron microscope (SEM) measurements. For the data shown in Fig. 3, the sample is held near the melting point in an attempt to understand melting behavior in small crystals.

Discussion

As mentioned above, the progress of the iterative fitting is monitored by calculating an rms error per pixel. For the fit shown in Fig. 3, this mean error per pixel is 10%. Examination of the original CXD pattern shows a background level of one to two photons per pixel, well away from the diffraction pattern itself. This is probably caused by liquid scattering that originates from smaller Pb crystals on the sample, which have lower size-dependent melting points. Additionally, the circular region of zero intensity is the result of removing the diffraction from a different crystal from this CXD pattern. Finally, the slight density gradient within the crystal is unexpected and may be an artifact from the partial coherence of the incident x-ray beam.

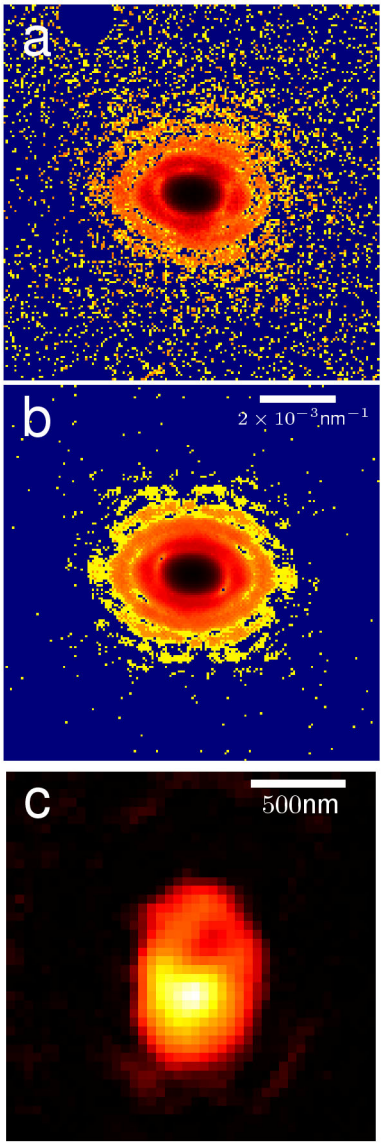

FIG. 3. Top a: 2-D slice through 3-D CXD pattern. Middle b: Reconstructed diffracted amplitude. Bottom c: Resultant real space density projected onto a plane through the crystal. The rms error between the data and the reconstruction is 10%.

Acknowledgments

The assistance of H. Hong and C. Benson of UNI-CAT was greatly appreciated. UNI-CAT is supported by the University of Illinois at Urbana-Champaign, Materials Research Laboratory (U.S. Department of Energy [DOE]; State of Illinois Board of Higher Education, Higher Education Cooperation Act; and National Science Foundation); Oak Ridge National Laboratory (DOE under

contract with UT-Battelle, LLC); National Institute of Standards and Technology (U.S. Department of Commerce); and UOP LLC. Use of the APS was supported by the DOE Office of Science, Office of Basic Energy Sciences, under Contract No. W-31-109-ENG-38.

References

[1] G.J. Williams, M.A. Pfeifer, I.A. Vartanyants, and I.K. Robinson, Phys. Rev. Lett. **90**, 175501 (2003).
[2] J.R. Feinup, Appl. Opt. **21**, 2758 (1982).